FILE

INTERNAL DOCUMENT 212

I.O.S.

pw 23

ork was funded by the Department of Trade and

Internal Document No. 212

[*This document should not be cited in a published bibliography, and is supplied for the use of the recipient only*].

NATURAL ENVIRONMENT RESEARCH COUNCIL

INSTITUTE OF OCEANOGRAPHIC SCIENCES

INSTITUTE OF OCEANOGRAPHIC SCIENCES

Wormley, Godalming,
Surrey GU8 5UB
(042-879-4141)

(Director: Dr. A. S. Laughton, FRS)

Bidston Observatory,
Birkenhead,
Merseyside L43 7RA
(051-653-8633)
(Assistant Director: Dr. D. E. Cartwright)

Crossway,
Taunton,
Somerset TA1 2DW
(0823-86211)
(Assistant Director: M. J. Tucker)

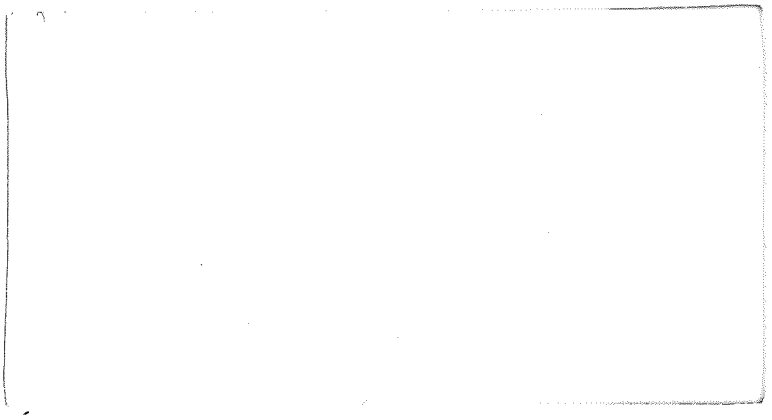

REPORT ON THE MEASUREMENT OF HIGH FREQUENCY SURFACE WAVES

By

J.A. Ewing, C.H. Clayson, K.G. Birch and R.W. Pascal

Institute of Oceanographic Sciences, Wormley, Godalming, Surrey, GU8 5UB

This work was funded by the Department of Trade and Industry

Internal Document No. 212

June 1984

1. Objective

To assess the capability of a laser doppler vibrometer for making accurate measurements of the energy spectrum of ripples in the frequency range from 4 Hz to about 8 Hz.

2. Introduction

The region of the wave spectrum between 4 Hz and 8 Hz is of importance in applications of remote sensing and for general scientific reasons.

High frequency waves play an important role in the use of radar scattering for the remote sensing of ocean wave parameters. Sea waves with a wavelength one-half that of the radar signal can result in significant backscatter by the mechanism of Bragg reflection (for the scatterometer on ERS-1, the relevant sea wavelengths giving Bragg reflection range from 3 cm to 7 cm). However, the interpretation of Bragg-scattered signals requires a knowledge of the long waves usually present in oceanic measurements as well as the spectral characteristics of the short waves.

In addition to these considerations, there is a need to understand the dynamics and properties of short waves. Wind-wave generation and the nonlinear energy transfer from short to long waves depend on processes occurring in the high frequency tail of the wave spectrum. Furthermore the dissipation of energy in a sea state and the process of wave breaking also depend on the spectral energy balance at high frequencies.

Most measurements of wind waves have been made in the gravity wave regime where surface tension is not important. However, for accurate measurements of ripples with frequencies greater than 4 Hz, it is not possible to use wave staffs due to the meniscus which forms around the sensor. Several non-intrusive optical methods are available for the measurement of the slopes of the ripples but most of these studies have been made in laboratory wind-wave channels where the processes being studied may not be representative of oceanic conditions.

The measurement of these short wavelengths in the presence of long waves is complicated by non-linear interactions. The most important one in the present context is the Doppler shift in the short waves due to the particle velocities in the long waves. It is easiest to explain this by an example. Suppose that there is a swell of 1 m crest-to-trough amplitude and with a period of 6.3 s ($=2\pi$s), then the horizontal particle velocities in the crests and troughs will be 0.5 m/s. This is the phase velocity of waves of about 3 Hz, whose frequency relative to a fixed wave probe will therefore temporarily drop to zero. It is possible to make an approximate correction for this only when the effect is small.

However, to get realistic conditions over the range of frequencies of interest, it is necessary to have a long enough fetch for equilibrium to be set up in the energy transfer processes in both the air and the water. Clearly there is a compromise between this and the generation of the long waves which make interpretation impossible. The fetch of approximately 1 km over deep water which was used in the present experiments is probably not far off the optimum for at least some conditions. The interpretation of ripple wave spectra is therefore simplified in measurements made on the reservoir due to the absence of long swell waves which are usually present in the ocean.

3. Review of previous work

The measurements of Burling (1955), made on Staines reservoir showed that the high-frequency tail of the wave spectrum varied approximately as frequency to the power -5. Phillips (1958) later argued on dimensional grounds that the high-frequency wave components were governed by wave breaking and were independent of wind speed. Thus at high frequencies the wave spectrum E is of the form

$$E(f) = \alpha\, g^2 (2\pi)^{-4} f^{-5} \qquad (1)$$

where α is a dimensionless constant and f is the wave frequency in Hertz. This "saturation range" has been observed in many studies up to a frequency of about 3Hz. Phillips (1977) has recently given the constant as $\alpha = 1.23 \times 10^{-2}$ with an uncertainty of about 10 per cent.

Following Lighthill (1978) we can define ripples as those wavelengths less than 7 cm for which surface tension effects are significant (the error in the gravity wave formula (see (2) below) is less than 3%, for wavelengths greater than 7cm). Capillary waves, which are not discussed in this report, may be defined as those waves with lengths less than 0.4cm.

For gravity waves the relation between frequency f and wavenumber k ($=2\pi/\lambda$, where λ is the wavelength) is given by

$$(2\pi f)^2 = gk \qquad (2)$$

For ripples, the dispersion relation becomes

$$(2\pi f)^2 = (g + Tk^2/\rho)k \qquad (3)$$

where T is the surface tension ($=0.074$ Nm^{-1}) and ρ is the density of water ($=1000$ kgm^{-3}).

The following table sets out the values of wave frequency and wavelength for gravity waves and ripples.

Table 1

Frequency Hz	Wavelength (cm)	
1.5	69.4	gravity waves
3	17.3	↕
4.8	7	
6	4.9	ripples
12	1.9	

Mitsuyasu (1977) measured the spectrum of high frequency waves up to about 10 Hz using a capacitance wave probe with a diameter of 0.35mm. The measurements were made from a tower off the coast of Japan. He found that the wave spectrum followed a frequency to the power-5 law up to 4 Hz. Above 6 Hz, there was a wind speed dependence in the wave spectrum, namely $E \alpha U f^{-4}$. However only one set of data at one speed, 8m/s, was analysed and also swell was present in the observations.

Kitaigorodskii (1981) discusses the measurements made by Leykin and Rosenberg made in a circular wind-wave channel up to a frequency of 6 Hz. In these experiments a long wave of period 4 sec was generated mechanically by a wavemaker and wind waves were produced by blowing air over the surface. It was found that wind-waves in the region 3-6 Hz were strongly dependent on the wind speed and such waves had an intermittent structure being concentrated at the crests of the long waves.

In a recent study made in the North Sea, Tang and Shemdin (1983) measured the slope of the short waves by means of a non-intrusive technique involving the refraction of light at the water surface. A strong wind speed dependence was found in the slope spectra for a range of wind speeds from 3m/s to 11 m/s and for frequencies greater than about 3 Hz.

Liu and Lin (1982) have compared measurements of high frequency wind waves using a wave gauge and a non-intrusive optical technique. They believe that wave staffs cannot measure short ripples with frequencies greater than 6 Hz due to the meniscus which forms on the wave probe. It appears from this study that the -5 power law obtained with wave staffs at high frequencies is the result of low-pass filtering caused by the meniscus.

4. Laser system and data logging equipment

A standard laser doppler velocimeter was hired from DISA (UK) for the month of February 1984. Briefly, this measures the doppler shift (f_D) of the frequency of a vertically incident coherent laser beam, backscattered from the water surface to give a precise measure of the vertical velocity of the water surface.

In order that both positive and negative values of f_D may be measured, the transmitted beam is frequency shifted relative to the reference beam with which the received light is heterodyned: this shift is achieved by a Bragg cell excited at 40 MHz. The optical heterodyne receiver output at frequency 40 MHz+ f_D is then mixed with a locally generated signal at a frequency 40 MHz+f_o where f_o is switch selectable in the range $\pm(1,2,\ldots,9)\times(10,100,1000)$ kHz. The mixer output component at f_o-f_D is then tracked by a phase-locked loop whose frequency tracking range is 0.1 f_T to f_T, where f_T is switch selectable in the range 10 kHz, 33.3 kHz, 100 kHz, 333 kHz, 1 MHz, 3.33 MHz and 10MHz.

For correct operation f_o is set to be greater than the maximum magnitude of f_D and f_T is set to approximately 2 f_o so that f_o-f_D remains within the tracking range 0.1 f_T to f_T at all times. Note that f_o can be positive or negative, the only effect being a reversal of polarity of the slope of the final analogue output: this output is given by $10\ (f_o-f_D)\ /f_T$ volts. After suitable scaling, anti-alias filtering and offsetting, the analogue velocity signal was logged by an Acorn BBC microcomputer, using the internal A/D convertor in 8 bit mode under control of a machine code interrupt handling routine, the interrupts being generated by an internal time at 50 Hz. The acquisition of data was begun on receipt of a signal from the microballoon dispensor (see Section 5) and, after 2048 data points had been acquired (over 40.96 seconds), the data were plotted on a VDU for examination. A cursor could be used to select short sections of the data for examination under magnified scale, this being necessary to detect any momentary dropouts in the laser system. Finally the cursor was used to select one or two good (1024 point) sections of the record for storage on floppy disc and subsequent processing as described elsewhere in this report.

(a) Calibration

The overall system was calibrated by introducing a fixed target into the laser beam, so that f_D was zero, and recording the digitised output (N_1) on the microcomputer. The offset frequency was then changed by a precise amount Δf_o and the digitised output noted again (N_2).

The calibration factor is then given by

$$\frac{\lambda \Delta f_o}{2(N_2 - N_1)} \quad \text{metre sec}^{-1} \text{ per digital unit}$$

where λ is the optical wavelength (6328Å or $6.328\ 10^{-7}$m)

A schematic of the laser doppler velocimeter system is given in Fig. 1.

5. Experimental techniques

The measurements were carried out from a platform at the Queen Elizabeth II reservoir at Hersham. The main tower structure, which is rigidly fixed to the bed of the reservoir has reinforced concrete legs which support four catwalks constructed from steel joists. At the centre of the catwalks is a concrete slab upon which a small brick laboratory is situated. A sensor platform is mounted below one of the catwalks on aluminium poles which can be adjusted in height by a winch system to cater for changes in the water storage level. Fig. 2 shows a schematic diagram of the platform.

(a) Vibration measurements

Since it was possible to sense vibrations of the catwalks in strong winds via the human body, quantitative measurements of these vibrations were made at the outset in order to assess the extent to which they would contaminate wave height measurements relative to the structure. A vertical accelerometer was, therefore, set at various positions on the catwalks and in the central laboratory and the analogue acceleration signal was recorded and analysed as discussed below. It was concluded from these measurements that vibration would not be a significant source of error in comparison to expected wave energy levels.

(b) Laser positioning

It was originally intended to keep the laser and associated electronic modules within the laboratory and to transmit the beam via a hole in the laboratory wall and a front silvered mirror (mounted at 45° to the vertical) on the edge of one of the catwalks. This involved a single way path length of approximately 6 metres. In practice it was found that the transmission loss was too high over this distance and the laser and mirror were, in fact, used on the lowered sensor platform, with a single way pathlength of 1.5 metres.

Previous experiments with the laser system in the IOS wave tank had shown that only a small fraction F of the incident beam was scattered by the water surface - most of the energy being specularly reflected or transmitted into the water. If the range is r and the receiving aperture has diameter d, then a proportion $d^2/8r^2$ of this scattered energy is received. Even at the shorter range, this proportion only amounts to 1.4×10^{-4}, giving a received power level of less than $^1/2$ microwatt for F=1. With a clean water/air

interface F is nearly zero and only occasionally would the receiving system function correctly, i.e. phase lock to the doppler frequency.

(c) Seeding media

To increase the backscatter from the water surface various additives were tried. These included milk, paint, aluminium powder and glass or ceramic microballoons of the type used as a low density filler in syntactic foams. The particles in milk and in paint (Titanium dioxide) scattered the light reasonably well, but dispersed too rapidly. They are probably better suited to flow measurements by laser doppler techniques since the backscattering was not restricted to the water-air interface. Aluminium powder was moderately successful under wave tank conditions but, since it relied on surface tension to keep it on the water-air interface, it was very difficult to achieve a reliable surface coating of it. Glass microballoons were the best seeding medium, followed closely by ceramic microballoons which gave a slightly lower backscatter, presumably due to absorption reducing the internally reflected light. Due to the high cost of the glass microballoons, the ceramic type were used (^{1}/10th the cost).

The microballoons are manufactured by passing small particles of ceramic containing a blowing agent through a flame, under closely controlled conditions. The particles then form hollow ceramic spheres with diameters mainly in the range 50-175 microns and with a wall thickness of, typically, 3.5 microns. In quantity, they have the appearance of very fine white sand and flow readily if poured out of a container. The true particle density is, on average, 0.6 so that the microballoons float with less than 60% submerged, depending upon the surface tension.

(d) Practical difficulties experienced

Whilst there was no difficulty in maintaining a continuous surface coating of microballoons in the wave tank, difficulties were experienced on the reservoir. The problems, which were not unexpected, were that

(i) the microballoons were to some extent blown by the wind between the dispensing vessel - which had to be kept above the highest wave crest - and the water. Since they had to be dispensed upwind of the laser beam, some blew through the beam causing intermittent errors.

(ii) once on the water surface the balloons drifted due to surface current and, possibly, windage so that continuous dispensing was required over the duration of a wave record - this used up large quantities of microballoons.

(iii) breaking waves would cause discontinuities in the surface coverage.

These problems limited the maximum wind speed in which the technique could be used satisfactorily. Even at low wind speeds, when an apparently good coating was present, unexpected signal dropouts would occur occasionally. It appeared that the dynamic range of the optodetector/phase locked loop system was very restricted. Since the electronics system was, presumably, designed to cover a wide range of applications and, in particular, had a much higher loop bandwidth than necessary for wave measurement, it is probable that more reliable operation could be achieved by circuit modifications. Since the equipment was hired, this could not be attempted. Agrawal (1984) at Woods Hole Oceanographic Institution has also noted the limited performance of the Disa 55N20 in tracking particles in water flow measurements and has developed improved techniques using spectral analysis and spectral peak detection

techniques. Some improvement in the microballoon dispensing technique could also be achieved.

6. Data analysis

The measurements discussed in the previous section were all recorded and analysed on the BBC Microcomputer. The analogue signals were converted to digital series, using the microcomputer. All the data were sampled at 50 Hz for 20.48 sec and then stored on floppydisks. Processing of the data on disk was then made using standard spectral analysis methods based on the use of the Fast Fourier Transform (FFT) over 1024 data points. Finally plots of the spectral data - platform motion, laser and wave staff - were viewed on a television monitor screen and hard copies obtained on a printer, together with the numerical results of the analysis.

(a) Platform motions

The output from the accelerometer was sampled at 50 Hz and acceleration spectra E_a were computed using the FFT over 1024 data points. Displacement spectra E_p were computed using the relation $E_p=E_a/(2\pi f)^4$ and averaged over frequency bands of width 2.4 Hz to yield spectral estimates with approximately 100 degrees of freedom.

'drop-outs' were discarded. The spectra of velocity, E_v, were computed using the FFT over 1024 data points. Displacement spectra were evaluated from $E=E_v/(2\pi f)^2$ and averaged over 20 harmonics to provide estimates at a resolution of 1 Hz with 40 degrees of freedom.

(c) Wave staff

The output from the wave staff is directly proportional to wave elevation. Spectral estimates were computed, as for the other measurements, to give estimates with a resolution of 1 Hz and 40 degrees of freedom.

7. Results

(a) Platform motions

Two sets of measurements were made in wind speeds ranging from 6 m/s to 13 m/s. It was found that most of the energy in the acceleration spectra lay in frequencies less than 0.8 Hz but there was a secondary spectral peak at about 6 Hz which could affect the measurements of wave energy at high frequencies obtained from the laser velocimeter. Table 2 sets out the results including an estimate of platform displacement in a band of width 2.4 Hz centred on 6 Hz. (Significant displacement is defined as four times the square root of the variance over the appropriate bandwidth).

Table 2

Day (Nov. 1983)	Record no.	Position of transducer on platform leg.	Wind speed (m/s)	Significant displacement at 6 Hz (cm)	Total significant displacement (cm)
16	7-10	5 m from end	6	0.8×10^{-3}	0.015
25	16-17	"	10-13	1.0×10^{-3}	0.02
"	18-20	3 m from end	"	2.0×10^{-3}	0.02
"	11-14	2 m from end	"	3.0×10^{-3}	0.02

This table shows that the platform motion increases with wind speed and also nearer the end of each platform leg.

Fig. 3 shows the platform motion spectra for record 10 (wind speed 6 m/s) and record 20 (wind speed 10-13 m/s) compared with laser wave measurements in light winds less than 1 m/s. Platform motion spectra are at least one order of magnitude smaller than the displacement spectra measured with the laser at the lowest wind speeds in the frequency range 4-12 Hz.

(b) Laser wave measurements

Laser wave measurements were only possible at low wind speeds less than 4 m/s due to the microballoon patch becoming broken up by breaking waves (see section 5). It also became increasingly difficult to deploy a continuous patch of microballoons for the 20.48 sec. necessary for a complete record as the wind speed increased. (Rain also had the affect of breaking up the microballoon patch). Many records were rejected due to drop-outs: those records which were suitable for analysis are detailed in the following table. The records are grouped together according to the range of wind speed.

Table 3

Group	Record number	Day (Feb. 1984)	Wind speed (m/s) & direction	Significant velocity (cm/sec)	Significant waveheight (cm)
	23	29	0.8,310°	5.8	0.7
A(0-1m/s)	24	"	<0.5,310°	5.3	0.3
	25	"	1.1,310°	12.7	0.8
B(1-2.5m/s)	12	13	2.0,040°	13.3	0.9
	13	"	1.4,040°	10.0	0.7
	26	29	4.0,310°	29.6	3.2
C(2.5-4m/s)	27	"	2.7,310°	23.9	2.3
	27a	"	2.7,310°	21.5	1.9

The significant values of the velocity and wave height were obtained from four times the square root of the variance of the spectrum over the whole frequency range. The wind speed and wind direction were measured at a height of 10m above the mean water level and an average value, over a period of about 30 sec. was taken at the same time as the laser wave measurements.

The results for groups A, B and C are plotted in Figs. 3-5. Logarithmic scales are used for both axes. Equation (1), for the equilibrium range spectrum with constant $\alpha=1.23\times10^{-2}$, is shown as a dashed straight line with gradient -5 on the plots.

The rounding error of the velocity signals, as sampled by the BBC microcomputer, corresponds to 0.014 cm/sec. this is equivalent to a 'noise' spectrum for displacement of about 2×10^{-9} cm^2/Hz at a frequency of 12 Hz. Thus the lowest spectral levels ($\sim10^{-7}$ cm^2/Hz) from the laser measurements shown in Fig. 3 are significant and are not the result of rounding errors in the data.

(c) Wave staff

An attempt was made to compare measurements from the wave staff with those from the laser vibrometer. It was not possible to obtain simultaneous measurements from both systems due to limitations of the BBC microcomputer, thus after sampling the laser system there was a delay of a few minutes before changing over to sampling the wave staff. Comparative measurements were made on two occasions but detailed inspection of the laser records in the laboratory showed that these records suffered from several 'drop-outs' previously undetected.

We have therefore taken the measurements with the wave staff when the wind speed was 4.1 m/s and compared these with laser record 26 which was taken under very similar meteorological conditions but on another day. Fig. 6 shows the wave spectra from the two systems together with the equilibrium range spectrum.

8. Discussion

There is considerable variability in the spectra at the lowest wind speed range of 0-1 m/s (Fig. 3). The spectral levels are above those of the platform motion so there should not be any contamination from this source.

For wind speeds between 1 m/s and 4 m/s (Figs. 4 and 5) the spectra decay more rapidly than f^{-5}. For frequencies greater than 3 Hz the spectrum varies approximately as f^{-7}, while for lower frequencies there is some indication of the spectrum approaching the Phillips' saturation range given by equation (1). There is also some evidence of an increase in the spectral levels for frequencies greater than 6 Hz in Group C (2.5-4m/s) compared to Group B (1-2.5m/s). It is possible that the microballoons may have contributed to the damping of the ripples. However, visual observations of the ripples both with and without surface seeding did not indicate any marked effect which could account for the spectral levels being lower than f^{-5} at frequencies greater than 3 Hz.

At the low wind speeds for which we have obtained results from the laser, it seems that the structure of the wave surface is different from that caused by active wind-wave generation. Wave breaking is known to change the characteristics of the sea surface when the wind speed exceeds about 5m/s; below this wind speed the surface is "smooth". The conditions of these measurements therefore are unrepresentative of the majority of sea states where

wave breaking is frequently observed.

Comparisons between the wave staff and laser wave spectra show that these are in good agreement up to a frequency of about 3Hz. Above this frequency there is more energy in the records taken with the wave staff. However, due to the meniscus which is present in intrusive wave measurement techniques, there are doubts about the ability of the wave staff to measure high frequency waves.

9. Conclusions and recommendations

The laser doppler vibrometer was only able to supply useful information on high frequency waves at low wind speeds up to about 4m/s due to limitations in maintaining an adequate patch of microballoons in higher wind speeds. In the wind speed range up to 4m/s there was no significant wind speed dependence at high frequencies up to 12Hz.

Due to the difficulties of maintaining a continuous patch of microballoons in the reservoir, we would like to carry out some further tests in the laboratory. The aim of these tests would be to compare the laser vibrometer and fine wire wave staff so as to determine the range of frequencies over which it is possible to make accurate measurements with the wave staff.

We would also like to investigate a possible new technique which makes use of the laser vibrometer but without the need to seed the surface with microballoons. G. Hassall of DISA has reported that, with a plane scattering surface placed below the water surface, a strong return signal is received by the laser. We believe with the use of a curved scattering surface we can minimize the distortions present with a plane surface so that the return signal is related to the wave profile.

10. References

Agrawal, Y.C., 1984. "A CCD chirp-Z FFT Doppler signal processor for laser velocimetry". J. of Physics, E, Scientific Instruments, 17, 458-461.

Burling, R.W., 1955. Wind generation of waves on water. Ph.D. thesis, University of London.

Kitaigorodskii, S.A., 1981. The statistical characteristics of wind-generated short gravity waves. In "Spaceborne Synthetic Aperture Radar for Oceanography" Ed. R.C. Beal, P.S. De Leonibus and I. Katz, Johns Hopkins University Press, 32-40.

Lighthill, J., 1978. Waves in fluids, Cambridge University Press.

Liu, H-T. and J.-T. Lin, 1982. On the spectra of high-frequency wind waves. J. Fluid Mech., 123, 165-185.

Mitsuyasu, H., 1977. Measurement of the high-frequency spectrum of ocean surface waves. J. Phys. Oceanogr., 7, 882-891.

Phillips, O.M., 1958. The equilibrium range in the spectrum of wind-generated waves. J. Fluid Mech., 4, 426-434.

Phillips, O.M., 1977. The dynamics of the Upper Ocean. Cambridge University Press.

Tang, S. and O.H. Shemdin, 1983. Measurement of high frequency waves using a wave follower. J. Geophys. Res., 88, 9832-9840.

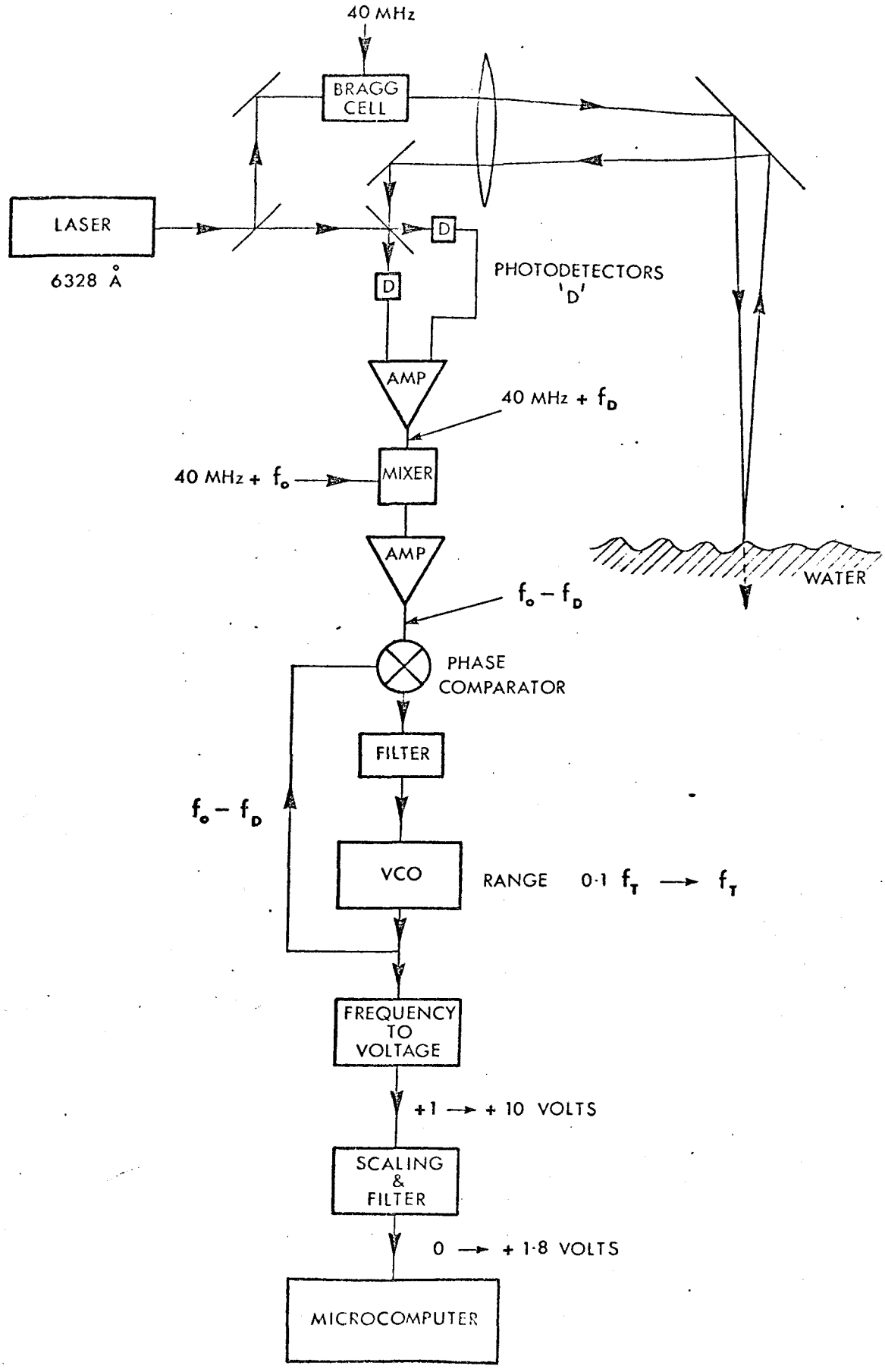

Schematic of Laser Doppler Velocimeter System

Fig. 1

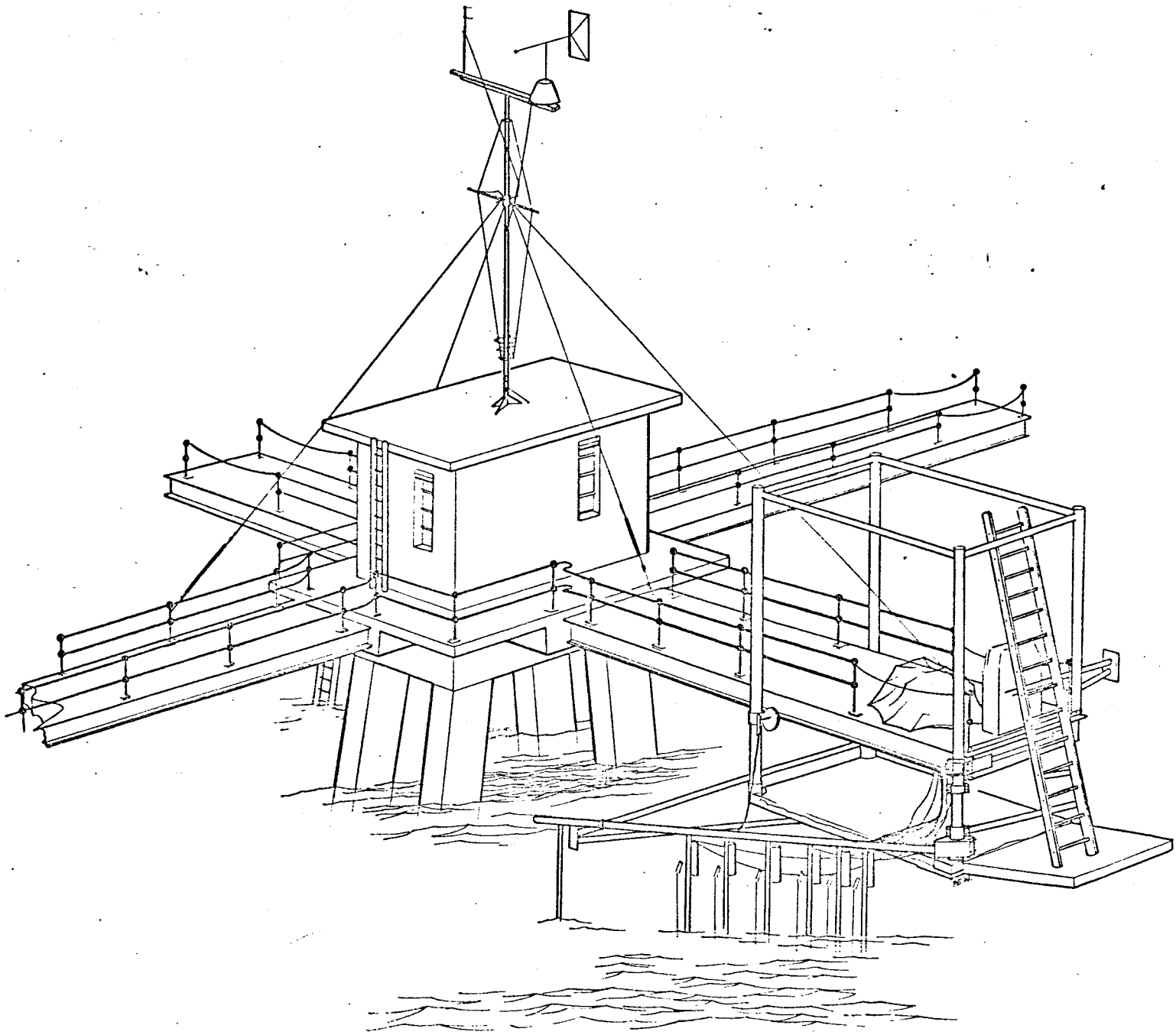

Fig. 2

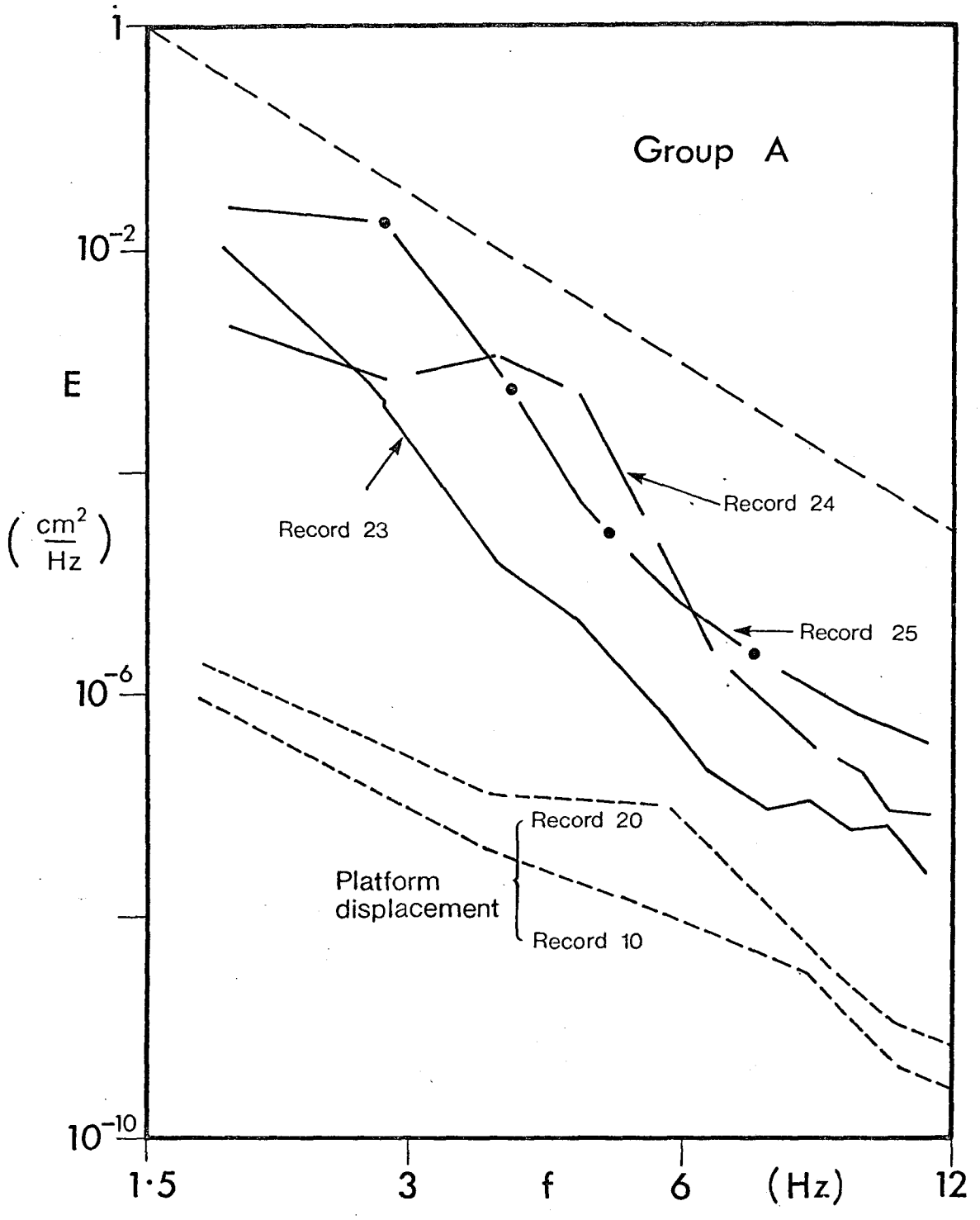

Fig. 3 Laser wave spectra for wind speeds in the range 0-1 m/s (Group A). Platform motion spectra are shown for comparison (see text). The dashed straight line is equation (1).

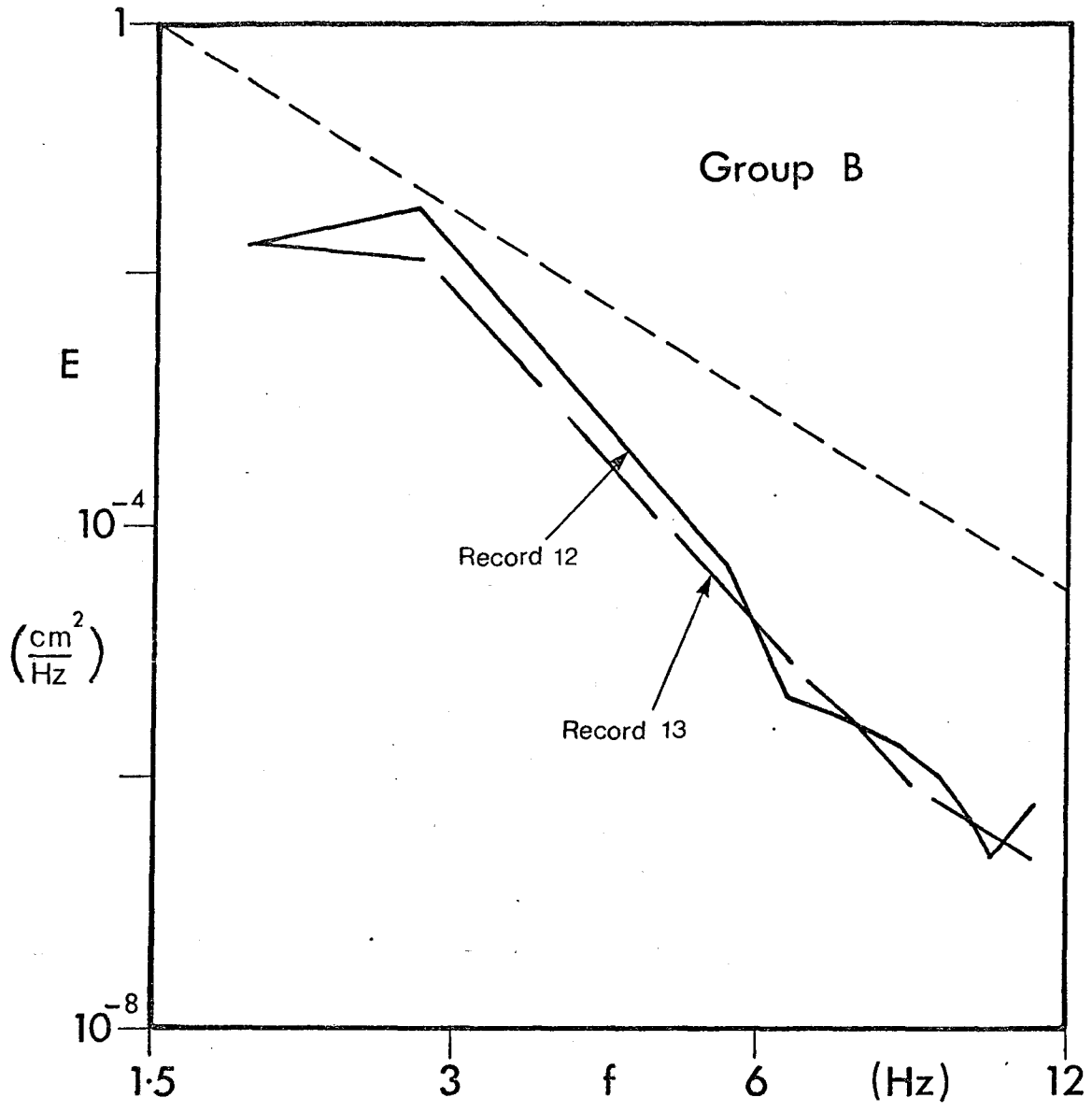

Fig. 4 Laser wave spectra for wind speeds in the range 1-2.5 m/s (Group B). The dashed straight line is equation (1).

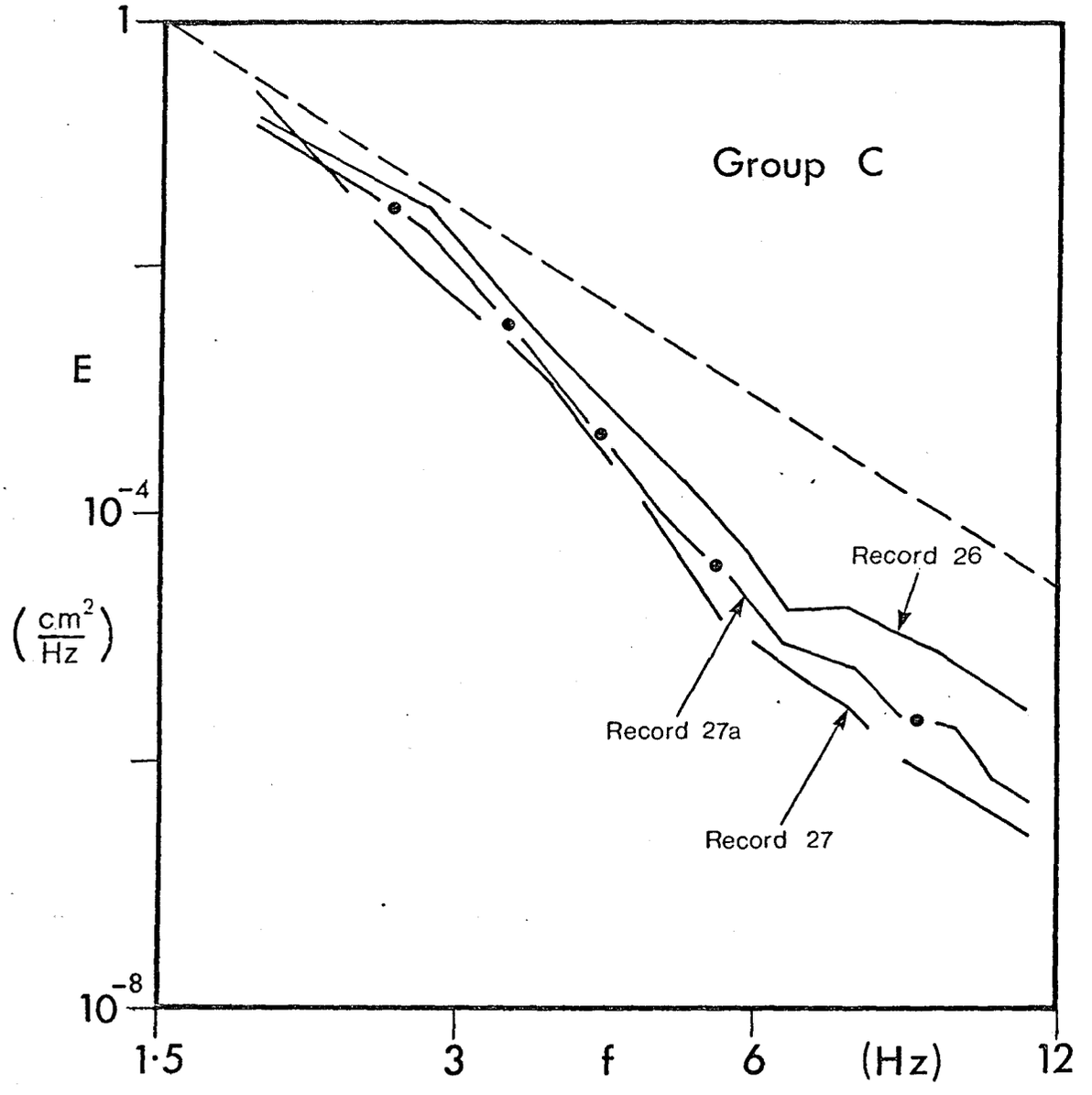

Fig. 5 Laser wave spectra for wind speeds in the range 2.5 - 4 m/s (Group C). The dashed straight line is equation (1).

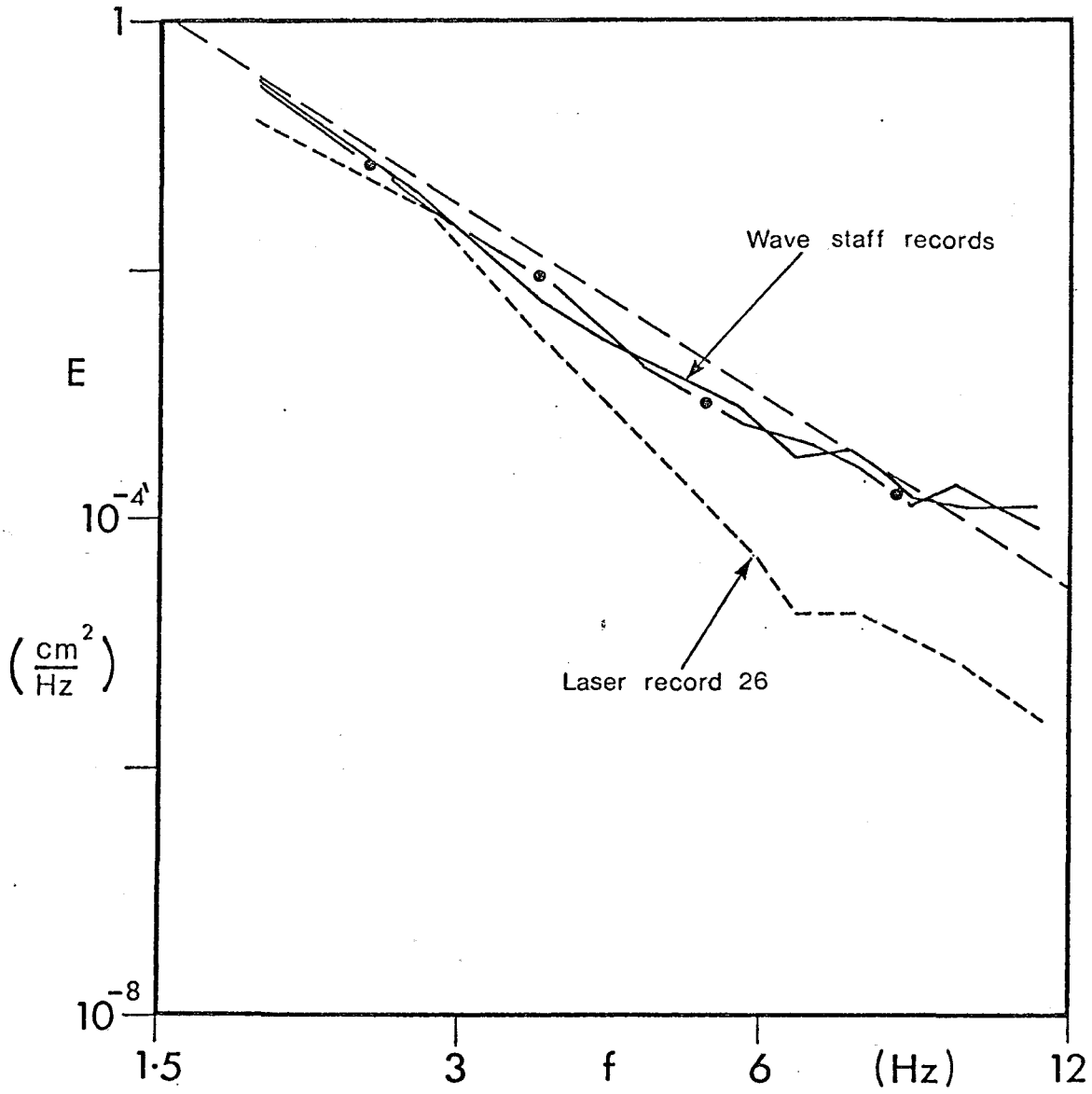

Fig. 6 Comparison of spectra obtained from laser and wave staff measurements. The dashed straight line is equation (1).